

FORCE GENERATION OF HEAT TRANSFORMABLE SHAPE MEMORY (NITINOL) IMPLANTS

AN ABSTRACT

SUBMITTED ON THE EIGHTH DAY OF MAY 2008

TO THE DEPARTMENT OF BIOMEDICAL ENGINEERING

IN PARTIAL FULFILLMENT OF THE REQUIREMENTS

OF THE SCHOOL OF SCIENCE AND ENGINEERING

OF TULANE UNIVERSITY

FOR THE DEGREE

OF

BACHELOR OF SCIENCE WITH HONORS IN BIOMEDICAL ENGINEERING

BY

\_\_\_\_\_  
JIBIN MATHEW MATTAPPALLY

APPROVED: \_\_\_\_\_

RICHARD B. ASHMAN, Ph.D.

\_\_\_\_\_  
RONALD C. ANDERSON, Ph.D.

\_\_\_\_\_  
MEGAN M. OHAR, M.S.E

## **ABSTRACT**

Approximately 6.8 million cases of bone fractures are reported in the United States each year that result directly from injury or other medical conditions (Cluett et al, 2007). While plates and screws are conventionally used for fixing complicated fractures, staple implants have gained more prominence in this field.

A subclass of staple fixation uses shape memory alloys with compositions such as Nitinol (alloy of nickel and titanium). Shape Memory Alloys (SMAs) have the ability to “remember” their pre-deformation shape. Nickel-Titanium (Nitinol) alloys will be the main focus of this thesis. The objective of this thesis was to perform compression force measurements that simulate the application of Nitinol staples to bone fracture.

Testing was performed on an MTS (Materials Testing System) machine, its accompanying TestWorks 4® software, and an Instron Environmental Chamber. Custom fixtures were created to hold the implants in place during the compression testing. The implants were transformed and forces were measured.

Analyzing the resulting peak and steady state values of load obtained for compression force measurement of each staple, it was observed that as staple size increased, average steady state value also increased. There was a non-linear relationship between the staple size and the average steady state value. When the sample was modeled as a beam in bending, there was still a non-linear relationship. Statistically significant results ( $p < 0.05$ ) were obtained which support the hypothesis that the mean steady state forces for each implant size were not similar to each other.

FORCE GENERATION OF HEAT TRANSFORMABLE SHAPE MEMORY (NITINOL) IMPLANTS

A THESIS

SUBMITTED ON THE EIGHTH DAY OF MAY 2008

TO THE DEPARTMENT OF BIOMEDICAL ENGINEERING

IN PARTIAL FULFILLMENT OF THE REQUIREMENTS

OF THE SCHOOL OF SCIENCE AND ENGINEERING

OF TULANE UNIVERSITY

FOR THE DEGREE

OF

BACHELOR OF SCIENCE WITH HONORS IN BIOMEDICAL ENGINEERING

BY

\_\_\_\_\_  
JIBIN MATHEW MATTAPPALLY

APPROVED: \_\_\_\_\_

RICHARD B. ASHMAN, Ph.D.

\_\_\_\_\_  
RONALD C. ANDERSON, Ph.D.

\_\_\_\_\_  
MEGAN M. OHAR, M.S.E.

## **ACKNOWLEDGEMENTS**

I would like to thank my thesis advisor, Dr. Rich Ashman for all his support and guidance throughout the formation of my thesis. I would also like to thank Megan Ohar (Masters in Biomedical Engineering, Tulane University, 2006) of InteliFUSE, Inc. for helping me get this thesis started in the first place. Finally, I would like to thank the Department of Biomedical Engineering of Tulane University for all that I've learnt over the past four years. The funding for my research was provided by InteliFUSE, Inc., New Orleans, LA.

# TABLE OF CONTENTS

<b>ACKNOWLEDGEMENTS .....</b>	<b>i</b>
<b>LIST OF FIGURES .....</b>	<b>iii</b>
<b>LIST OF TABLES .....</b>	<b>v</b>
<b>CHAPTER 1: INTRODUCTION.....</b>	<b>1</b>
<b>CHAPTER 2: BACKGROUND .....</b>	<b>3</b>
2.1 Fixing broken bones .....	3
2.2 Bone Healing .....	4
2.2.1 Wolff’s Law .....	5
2.3 Bone Staples.....	5
2.4 Shape Memory Alloys .....	6
2.4.1 Brief History of Nitinol.....	6
2.4.2 Properties of Nitinol.....	7
2.4.2.1 Shape Memory .....	7
2.4.2.2 Biocompatibility .....	10
2.4.3 Applications of Nitinol .....	10
2.4.3.1 Implants .....	10
<b>CHAPTER 3: MATERIALS AND METHODS .....</b>	<b>12</b>
3.1 Materials .....	12
3.1.1 Testing Equipment .....	12
3.1.2 Custom Fixtures .....	13
3.1.3 Implants and thermo-activators.....	15
3.2 Methods.....	16
<b>CHAPTER 4: RESULTS .....</b>	<b>18</b>
<b>CHAPTER 5: DISCUSSION .....</b>	<b>20</b>
<b>CHAPTER 6: CONCLUSION.....</b>	<b>22</b>
<b>APPENDIX I: LOAD VS. TIME GRAPHS .....</b>	<b>23</b>
<b>APPENDIX II: MEASURED EXPERIMENTAL VALUES.....</b>	<b>30</b>
<b>APPENDIX III: PROOF OF NON LINEAR RELATIONSHIP .....</b>	<b>32</b>
<b>REFERENCES.....</b>	<b>33</b>
<b>BIOGRAPHY .....</b>	<b>35</b>

## LIST OF FIGURES:

Figure 1.....	3
Examples of invasive fracture fixation methods: (a) screws and plates, and (b) intramedullary nail inside the bone and fixed with screws (www.bonefixator.com).	
Figure 2.....	8
A microscopic view of the shape memory process (Wayman et al, 1990).	
Figure 3.....	9
The Martensite-Austenite Transformation. Due to temperature change, mechanical properties and crystal structure of the metal are altered (Kujala, 2003).	
Figure 4.....	12
Nitinol Compression Staples: Formation, insertion, and compression (Mereau, 2006).	
Figure 6.....	13
The MTS (Materials Testing System) Device used for force generation of Nitinol implants.	
Figure 7.....	14
The Instron Environmental chamber used to observe changes in staples over a range of temperatures	
Figure 7.....	15
Fixtures for compression testing of Nitinol implants	
Figure 8.....	15
Implants held by fixtures in environmental chamber	
Figure 9.....	16
Available list of medical implants for experiment	
Figure 10.....	17
Intelifuser: A cordless thermo-activator	
Figure 11.....	19
Steady state analysis of small, medium, and large implants	
Figure A.....	23,24,25
Tests #1-5 for compression of small implants	

Figure B.....	25,26,27
Tests #1-5 for compression of medium implants	
Figure C.....	28,29,30
Tests #1-5 for compression of large implants	
Figure D.....	33
Proof of non-linear relationship of sample when modeled as beam in bending	

## LIST OF TABLES:

Table 4.1: Mean steady state and peak load values .....	19
Table A: Measured Experimental Values of Small Implants (9x6x6 mm) .....	31
Table B: Measured Experimental Values of Medium Implants (15x12x12 mm) .....	31
Table C: Measured Experimental Values of Large Implants(30x30x30 mm).....	32

## CHAPTER 1: INTRODUCTION

A fracture is defined as any kind of event where the bone breaks. There are approximately 6.8 million cases of various bone fractures in the United States every year (Cluett et al, 2007). Fractures can result from injury or through various medical conditions that weaken the bone such as osteoporosis.

Fractures are classified as open, closed and comminuted (multi-fragmentary), or simple. There is no damage to the skin in closed fractures, while in open fractures there is possible exposure to contamination due to open wounds. In comminuted fractures, the bone splits into multiple parts, while in simple fractures the fracture occurs along one line and the bone splits into two pieces.

The branch of surgery that deals with fixing fractures and other musculoskeletal disorders is orthopedic surgery. One in seven Americans has a musculoskeletal impairment that must be dealt with surgically. In the United States, orthopedic surgeries cost around \$215 billion annually (Praemer et al, 1999). In orthopedic surgery, there are basically two goals: realign the bone pieces and hold them in place while fusion occurs. Many fractures can be fixed without internal fixation, often using casts or other external fixation. In some cases, further intervention is required which usually results in a surgery to install internal fixation devices like plates and screws to aid in fusion. Plates and screws are commonly used to resolve fractures but staple implants have gained traction as a simpler and potentially cheaper method. There are two basic varieties of staple implants: static and shape transformable.

Shape Memory Alloys (SMAs) offer the ability to “remember” their pre-deformed shape. There are different versions of SMAs but in this thesis, the focus will be on Nickel-Titanium (Nitinol) alloys.

The objective of this thesis is to measure the forces that are generated by various shape memory Nitinol implant staples. Specifically, the forces generated by the implants will be measured in confined compression. During this application of force, the implant is transformed from the martensite phase to austenite phase. This study aims to analyze peak and steady state forces and the load for the implant's transformation cycle.

## CHAPTER 2: BACKGROUND

### 2.1 Fixing broken bones

In the treatment of fractures, the main objective is to ensure that after healing, the injured part maintains its function. This is accomplished by restoring the fractured pieces of bone to their natural positions and maintaining this position while the bone fuses. In simple fractures, a plaster cast is used to hold the bones in the correct position while also immobilizing the joints above and below the fracture. If surgery is required, various combinations of nails, wires, plates, or screws are used to directly hold the bones together. For internal fixation, the implants are attached directly to the bone during the healing period, and share the load with the bone by acting as a splint (Figure 1, left). In the case of some severe fractures, a combination of internal and external fixation is required (Figure 1, right).

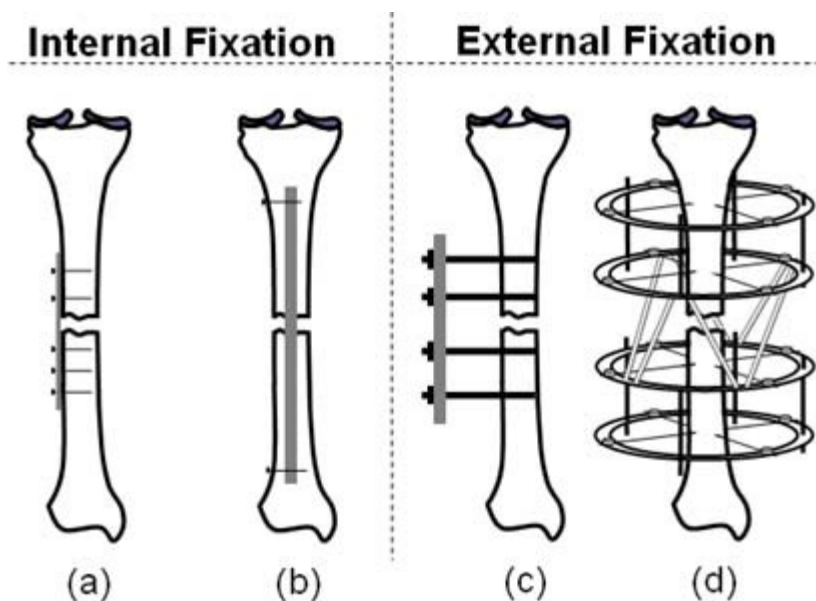


**Figure 1:** Examples of invasive fracture fixation methods: (a) screws and plates, and (b) intramedullary nail inside the bone and fixed with screws ([www.bonefixator.com](http://www.bonefixator.com)).

There are many advantages to using internal fixation devices. They provide excellent control over the position of bone segments, increased stability and rigidity, and early usage of joints and

muscles. Disadvantages include the risks of the surgical procedure to install the devices and “stress shielding” which can occur if the internal fixation device carries too large a portion of the bone’s load. Bone actively remodels in the presence of the stress applied. Most stress shielding leads to delayed union and poor bone formation since the bone does not see the appropriate stress levels. Additionally, a new fracture could also be formed at the ends of the implant due to high stiffness of the plate. When plates are used, the fracture heals mostly by primary cortical healing.

## 2.2 Bone Healing

In order to understand how fixations repair fractures, it is important to understand the process of fracture healing. There are five main stages of bone fracture healing:

- Induction – In this stage, a fracture hematoma is formed first after which inflammatory cells appear approximately 48 hours after the fracture.
- Inflammation – This stage begins with the influx of inflammatory cells, after which bone and cartilage production signal its end.
- Soft Callus Formation – This stage is characterized by bone and cartilage tissue development; the cessation of appreciable fracture motion occurs at the end of it.
- Ossification – Endochondral ossification occurs at this stage and is characterized by the conversion of the soft callus into woven bone.
- Bone Remodeling – This stage is the conversion of woven bone to lamellar bone, restoring the medullary cavity and bone geometry. The bone is finally remodeled into its final shape that resembles the original bone shape and strength.

The idea of remodeling is summarized as Wolff's Law (Kenneth et al, 2002) which basically states that the stresses applied on bone during their normal use cause the bone to get stronger, especially in the direction opposing the forces.

### 2.2.1 Wolff's Law

In 1892, Julius Wolff formulated the 'Law of Transformation of Bone' which stated that "formation of bone takes place wherever stresses of pressure and tension are caused in bone, be it by pressing or pulling forces" (Kushner, 1940). It states that bones of a healthy animal will undergo remodeling based on the various loads under the given loading conditions. The remodeling will result in an optimal architecture for the bone. Hence basically stated, Wolff's Law says 'form follows function'. If bone loading increases, the bone will increase its strength over time to be able to withstand increased loading. Since Julius Wolff, a number of researchers have further proven his research and shown that increased bone mass occurs with increased stresses on the bone (Kushner, 1940). This is clearly illustrated when the leg bones of a normal person are observed as compared to those of a wheel chair bound paraplegic. The bones of a normal person are exposed to stresses during daily activities and correspondingly are much stronger than those bones that experience no stresses.

### 2.3 Bone Staples

Since 1906, bone staples have been used in the United States for foot procedures. The advantages of staple fixation include dynamic compression, good approximation of fragments, avoidance of pin-tract infections from exposed hardware, and less operating time in comparison to screws and plates (Mereau et al, 2006). In the past, bone staples helped maintain bone

alignment but did not provide compression, were too bulky, had a tendency to become loose, and demonstrated an inconsistent fixation quality.

The application of compression staples requires four steps: fracture reduction and pre-drilling implant holes, implanting the staple, seating the staple and applying heat for compression (Mereau et al, 2006). Presently, staple fixation and stability has been improved by the composition of the metal. An example of temperature controlling the shape of a metal alloy is Nitinol.

## **2.4 Shape Memory Alloys**

All elemental metals have distinctive properties which can be enhanced or detracted when combining metals to form alloys. A special group of alloys called shape memory alloys (SMAs) show the unique ability to change shape under certain conditions. At low temperatures, these materials can be deformed in such a way that they will remain stable until heated, at which time they will return to their original shape. The study of materials science has shown that what actually happens to these metals is a shifting of their crystallographic structure. At high temperatures, the crystal structures are known as “austenite” and at lower temperatures, “martensite”.

### **2.4.1 Brief History of Nitinol**

While working on various alloy systems for his materials project in 1959, William J. Buehler, a metallurgist at the Naval Ordnance Laboratory (NOL), found that an equiatomic nickel-titanium alloy had more significant impact resistance and ductility than other alloy systems (Kauffman et

al, 1996). He concentrated on this and named his discovery NITINOL (**N**ickel **T**itanium **N**aval **O**rdnance **L**aboratory).

After additional studies, he discovered various tendencies of nitinol that hinted to its shape memory property. During a presentation of his findings, someone accidentally applied heat to a strip of bent nitinol and observed that it stretched back into its original shape. This discovery was the start of numerous advances and research in the field of nitinol.

## 2.4.2 Properties of Nitinol

### *2.4.2.1 Shape Memory*

Shape Memory is the ability of certain materials to remember their original shapes. During this process, the material undergoes a martensitic-to-austenitic transformation, a crystalline to solid phase change (Figure 2) which is the basis for the memory effect. Martensitic transformations are “displacive transformations” which do not need long range movements. In this transformation, the atoms are rearranged into a new and more stable crystal structure while the chemical nature of the matrix does not change (Wayman et al, 1990). These processes are also first order transformations in which heat is liberated when martensite is formed. There is a hysteresis associated with this transformation (the transformation temperatures differ upon heating and cooling) and a temperature range over which martensite and austenite coexists.

Nitinol undergoes only a shape change of martensite, unlike in steel where the volume changes, too. The shape of the new phase or the surrounding austenite must be changed to accommodate the new structure. This can happen by two main mechanisms: “slip” (a change that involves break in the crystal structure which causes the volume and the shape to change) or “twinning” (a shifting of the crystal structure which causes the shape to change but maintains its

original volume, see Figure 2). While slip is a permanent process and a common accommodation mechanism in several martensites, twinning is reversible and can accommodate shape, but not volume, changes. Twinning must be the dominant accommodation process for shape memory to occur since it is fully reversible (Wayman et al, 1990).

Martensite can form from austenite in various ways but there is only one way for it to return to the austenite structure. The foundation for the shape memory effect is based on this basic geometric concept.

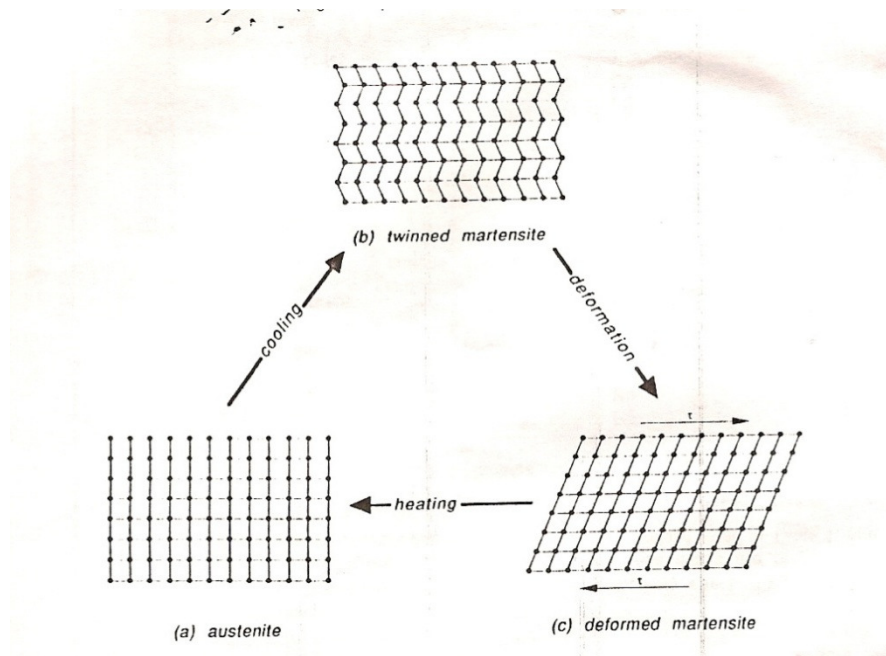


**Figure 2:** A microscopic view of the shape memory process (Wayman et al, 1990).

In Figure 2(b), twinned martensite is formed after austenite (Figure 2(a)) is cooled. It is deformed without undergoing a shape change (Figure 2(c)) by moving the twin boundaries. Upon heating the twinned or deformed martensite, only austenite can be formed again.

The martensite-to-austenite transformation can be further explained in Figure 3. The original shape is created by heating the alloy to a temperature well above  $A_f$  (final austenite temperature). At this point, the transformation to austenite is complete and the material is

restrained to the desired shape for a certain time period. There is no change in the specimen shape when it is cooled from above  $A_f$  to below  $M_f$  (final martensite temperature). When deformed below  $M_f$ , it remains in this state until heated. In the context of orthopedic application,  $A_s$  (start austenite temperature) can be considered as the body temperature. So if the implant is heated to above this body temperature, shape recovery begins and is then completed at  $A_f$ . After completed shape recovery at  $A_f$ , there is no shape change when the specimen is cooled to below  $M_f$ . Thus, the reactivation of shape memory can only take place by the re-deformation of the martensitic specimen (Wayman et al, 1990). In Figure 3,  $M_s$  is the start martensitic temperature and the  $H$  (hysteresis) is the difference between the transition temperatures upon heating and cooling. The shape memory effect occurs only once and is referred to as a “one way shape memory”.

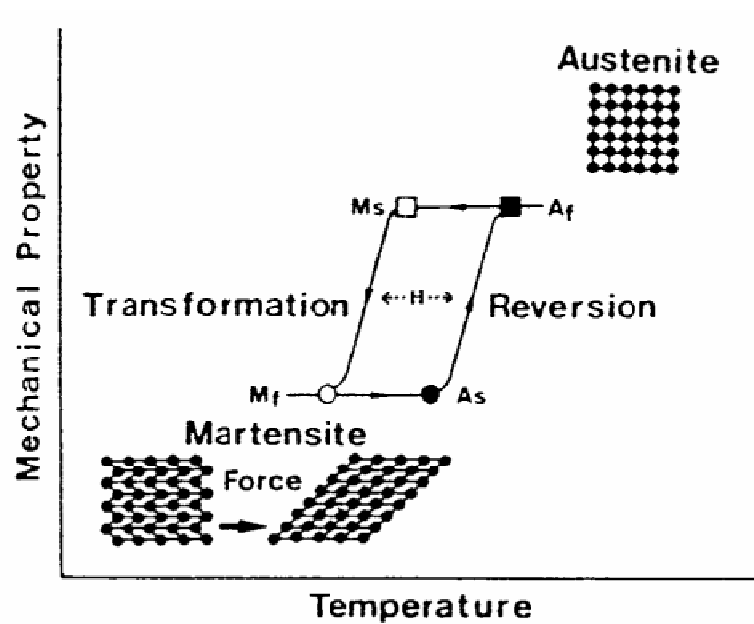


**Figure 3:** The Martensite-Austenite Transformation. Due to temperature change, mechanical properties and crystal structure of the metal are altered (Kujala, 2003).

#### *2.4.2.2 Biocompatibility*

“Biocompatibility” is a material’s ability to remain biologically innocuous during its functional period inside a living creature (Machado et al, 2003). Two main factors that determine biocompatibility of a material are the material induced host reactions and the degradation of the material in the body environment. Titanium is well tolerated and known to have excellent biocompatibility and corrosion resistance due to the stable titanium oxide ( $\text{TiO}_2$ ) layer that naturally forms on its surface. Nickel, on the hand, is known to be toxic to humans and can cause severe allergies. Nitinol’s surface layer is primarily composed of stable titanium oxide but can contain small amounts of nickel oxides ( $\text{NiO}$  and  $\text{Ni}_2\text{O}_3$ ) (Kujala, 2003). Medical-grade nitinol (as specified by ASTM F2063-05) is considered to be suitable for implant use and have excellent biocompatibility in bone tissue largely due to its passive oxide layer (Ryhanen et al, 1999).

### 2.4.3 Applications of Nitinol

#### *2.4.3.1 Implants*

Various factors on which staple fixation depend are: leg length and width, cross-section geometry, angle of insertion, bone density, and power versus hand-driven technique (Mereau et al, 2006).

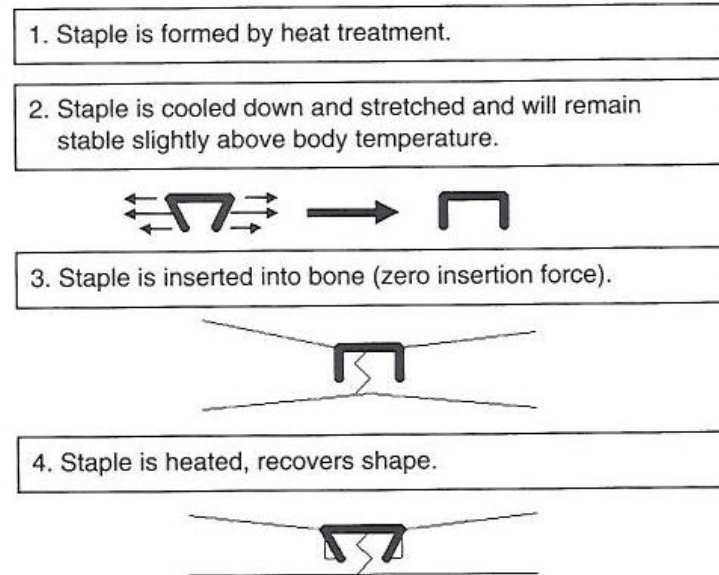


**Figure 4:** Nitinol Compression Staples: Formation, insertion, and compression (Mereau, 2006).

The Nitinol compression staples in Figure 4 were first introduced in 1983. Most are based on same principle: A nitinol staple is first formed with nickel and titanium and by various heat treatments. The staple is then cooled down and stretched and will remain stable slightly above body temperature. The arms of the staple are then specially inserted into holes drilled in the fractured bone (see Figure 4.3). When the staple is then heated it will restore to its original shape, leading to compression between the fragments (see Figure 4.4). These forces created by the staple prongs apply dynamic compression to the bone fragments once the implant has been heated. The Nitinol Transition temperature level is around 42°-52° C (Mereau et al, 2006) which is well below established tissue necrosis temperatures (Moritz et al, 1947).

## CHAPTER 3: MATERIALS AND METHODS

### 3.1 Materials

#### 3.1.1. Testing Equipment

A Materials Testing System (MTS) Device (Model # 1122, Eden Prairie, MN) utilizing TestWorks 4® software (version 4.05) was used for compression testing of the implants (Figure 5). A 1000lb reversible load cell was installed and used in conjunction with an Instron environmental chamber (Norwood, MA).



**Figure 5:** The MTS (Materials Testing System) Device used for force generation of Nitinol Implants

The environmental chamber (Model# 3111, Figure 6) ranges in temperatures from -129° C (-200° F) to 1000° C (540° F) and it helps maintain a constant temperature throughout the testing.



**Figure 6:** The Instron Environmental chamber used to observe changes in staples over a range of temperatures.

### 3.1.2 Custom Fixtures

Fixtures made of polyethylene were created to hold the implant in place during the experiment (Figure 7 & 8). The grips were drilled through 9/64” to fit the legs of the large and medium implants and 1/16” to fit the legs of the small implants.

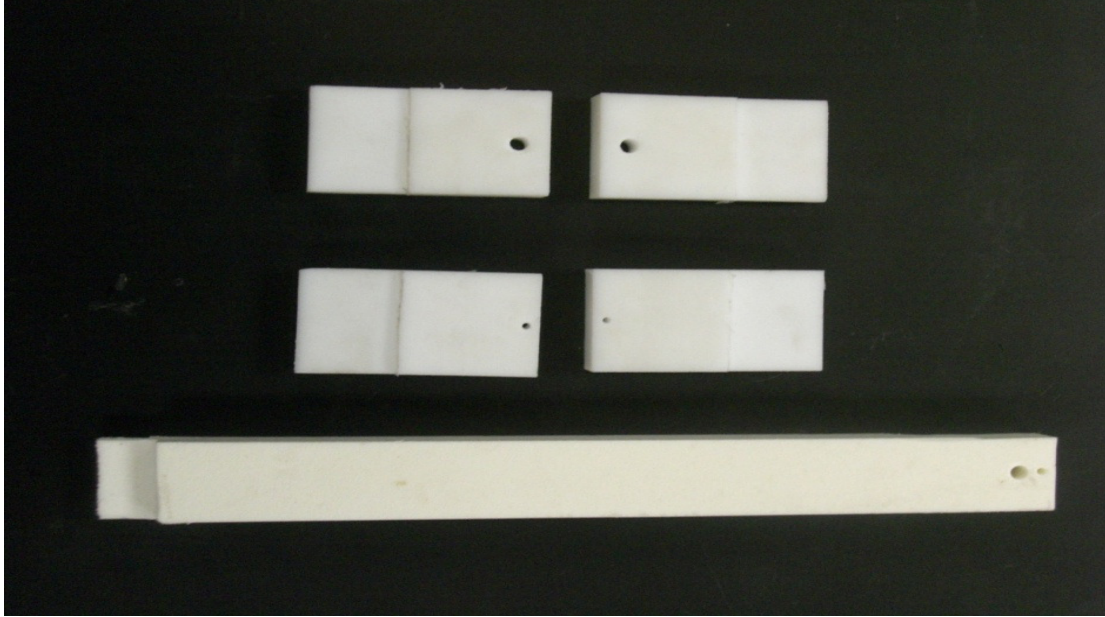


**Figure 7:** Fixtures for compression testing of Nitinol implants

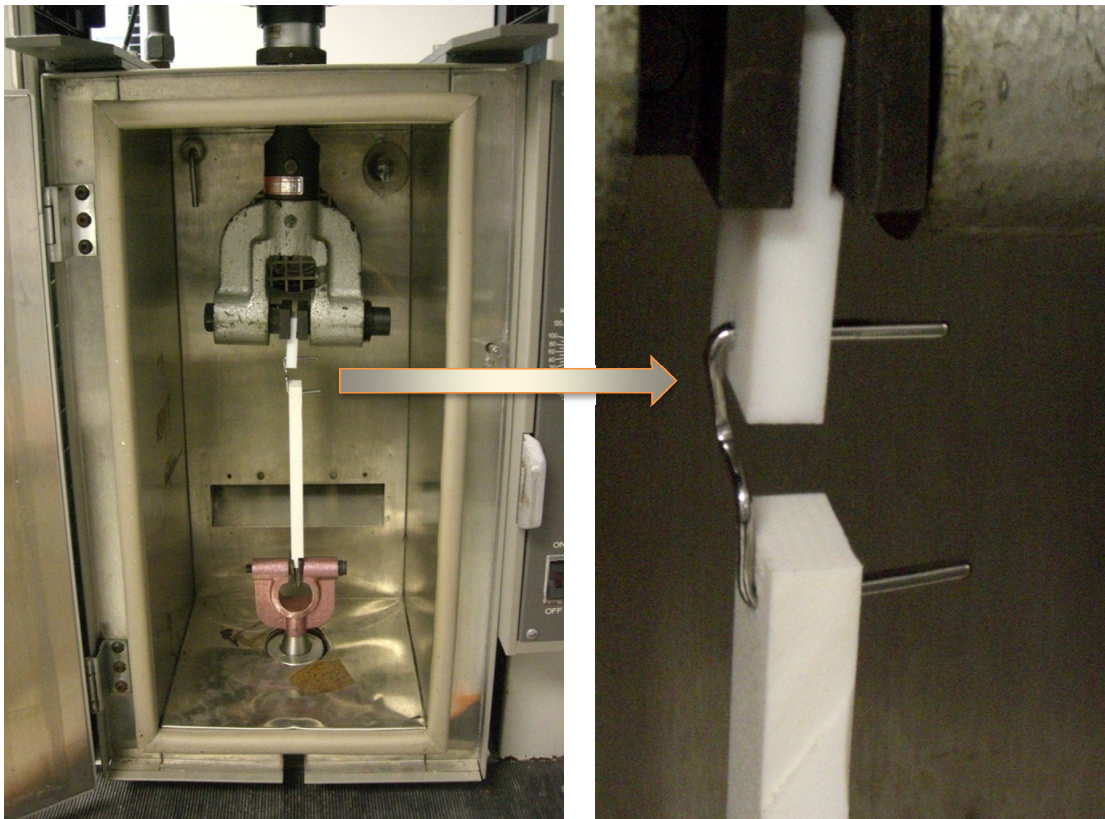


**Figure 8:** Implant held by fixtures in environmental chamber

### 3.1.3 Implants and thermo-activators

Implant sizes are designated both by the geometric orientation (bridge x leg x leg) and gauge of nitinol wire. Five each of three different sizes were used (Figure 9):

- Small: 9x6x6 mm (1.2x1.2mm gauge); Lot# 1408/11
- Medium: 15x12x12 mm (1.5x1.5mm gauge); Lot# 1408/10
- Large: 30x30x30 mm (2x3mm gauge); Lot# 1408/7

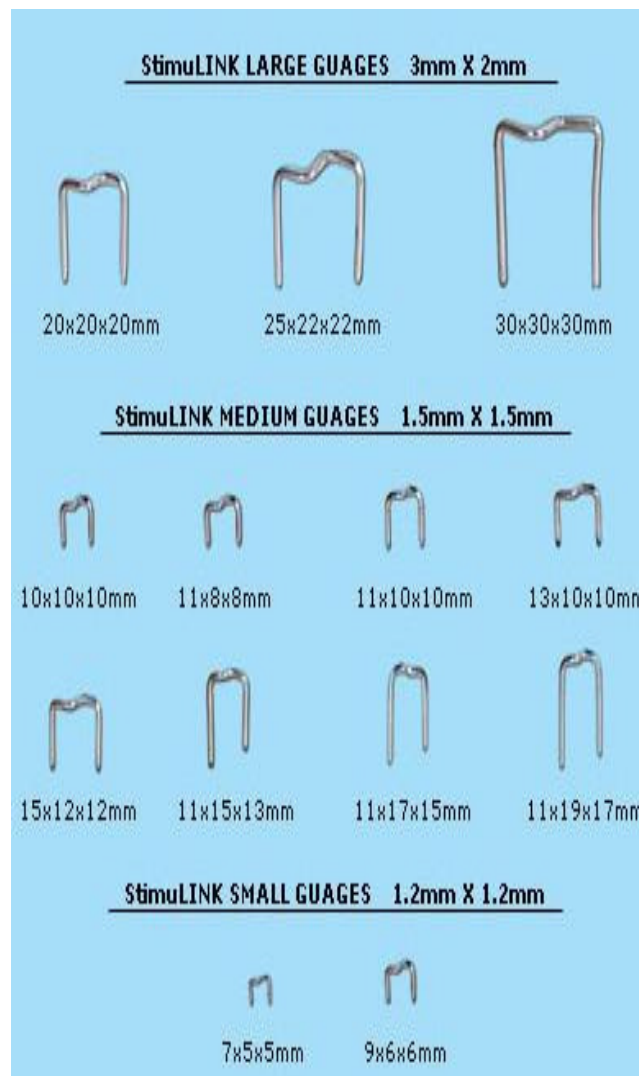


**Figure 9:** Available list of medical implants for experiment

The electrodes of a cordless thermo-activator, otherwise known as an Intelifuser (InteliFUSE, New Orleans, LA) help activate implant compression and heat the implant in seconds (Figure 10). It consists of a single AA battery and a switch which helped run current through the staple and helped to resistively heat the back of the staple.



**Figure 10:** Intelifuser: A cordless thermo-activator

### **3.2 Methods**

The environmental chamber was set to 37° C for a minimum of 15 minutes prior to the start of any test. The top custom fixture was installed, lifting the environmental chamber to install the bottom custom fixture. The temperature was checked to ensure that the chamber had reached 37° C prior to inserting the implant. A single implant was inserted into the fixture. The machine was zeroed and preloaded to 0.5lbf tension and test speed to 0 in/min before starting the test. Time and load results were measured and peak and steady state values were calculated while

an Intelifuser was applied to the implant. The electrodes of the Intelifuser were placed at the center of the bridge on all small gauge implants and two activation cycles, one at each implant shoulder, for medium and large gauge implants. All cycles lasted 30 seconds or longer to ensure full transformation. The door of the chamber was immediately closed after activation and left for a minimum of 150 seconds until steady state loads were observed. The test was repeated for additional implants and the fixtures were changed as required by the implant size.

## CHAPTER 4: RESULTS

For the force generation of five each of the small, medium, and large staples, load (pound force) vs. time (seconds) graphs were obtained. The most important observation to be made from these graphs is the steady state value of the implant loads after several minutes, especially the difference between large, medium, and small sizes.

Figure 11 below shows one sample test for each implant gauge. The green line corresponds to small implants, red to medium implants, and blue to large implants. Note that the steady state value increases significantly as the gauge increases. The steady state values obtained in this experiment fell in the expected ranges for both small and large implants while the medium was slightly lower than expected.

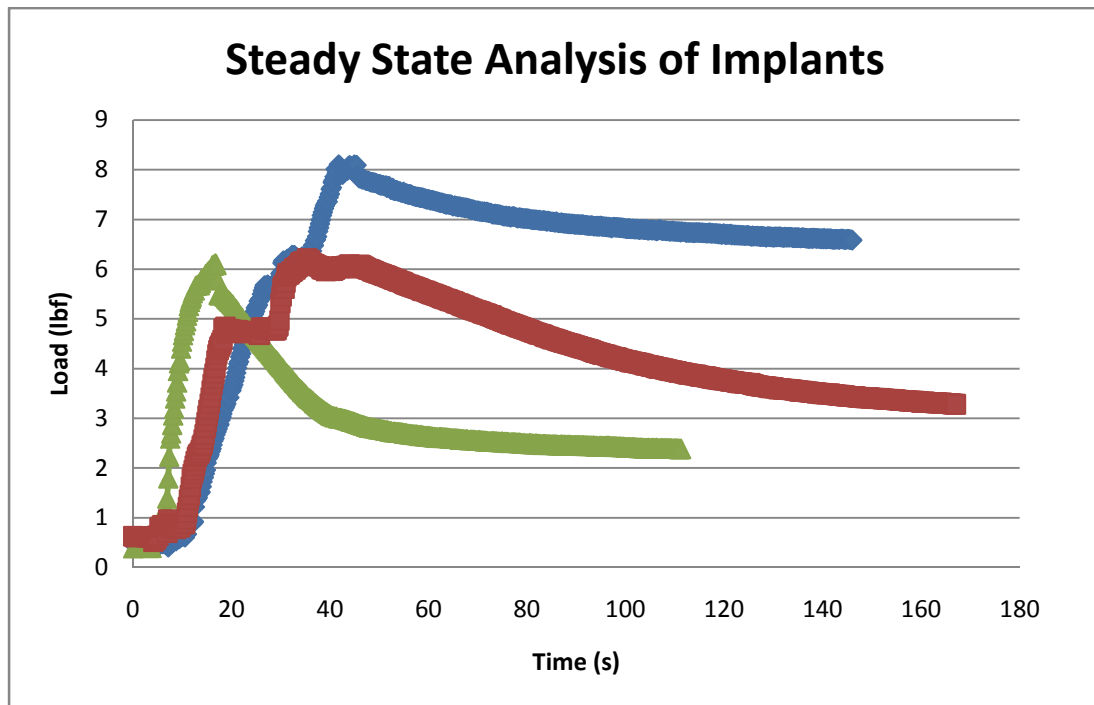


Figure 11: Steady state analysis of small, medium, and large implants

Average peak and steady state values for measured loads of small, medium, and large implants are displayed in Table 4.1. Individual graphs for each of the 15 experiments as well as individual experimental values are listed in Appendix I and II.

**Table 4.1:** Mean steady state and peak load values

<b>Size</b>	<b>Cross-section (mm)</b>	<b>Mean peak value (lbf)</b>	<b>Mean steady state value (lbf)</b>
Small	1.2 X 1.2	5.91	2.79 ± 0.28
Medium	1.5 X 1.5	6.18	3.62 ± 0.17
Large	2 X 3	8.72	7.34 ± 0.45

## CHAPTER 5: DISCUSSION

Analyzing the graphs for all 15 experiments reveal steady state values that can be maintained at body temperature after insertion of an implant. This steady state value corresponds to the amount of dynamic compression forces applied to the bone fragments during fracture healing. Each graph shows a peak value at which point the implant is recovering from the austenitic phase and cannot maintain that force for a certain period of time. Rather than using the brief peak value, the steady state force can be maintained at body temperature and is the appropriate measure for future studies in compressive forces during bone remodeling.

Analyzing the resulting peak and steady state values of load obtained for compression force measurement of each staple, it is observed that as staple size increases, average steady state load value also increases. Steady state loads were on average 47% of the peak load for small implants, 58.6% of the peak load for medium implants, and 84.2% of the peak load for large implants. It is believed that this is because for the large implants, there is less recovery from the austenite or high temperature phase than smaller implants. It is believed that this could be due to the specific heat treatments of large implants compared to small implants.

The mean steady state values of load for small, medium, and large implants are displayed in Table 4.1. The relationship between cross sectional area and mean steady state force was expected to be linear. Bending characterizes the behavior of a structural element (in this case, the implant) subjected to an external load applied perpendicular to the axis of the element. A structural element subjected to bending is known as a beam. After modeling this experiment by beam in bending (see Appendix III), it was discovered that this relationship was in fact non-linear. This is likely due to the slight variations in heat treatment of the smaller wire from which staple are made compared to the larger wires.

Finally, an ANOVA (ANalysis Of VAriance) test was used to test for differences among the sample size, mean steady state values, and steady state standard deviation using the F distribution. Our null hypothesis was that the steady state means were the same for each implant size. After the ANOVA, we determined that  $p < 0.05$  which means that there is a less than 5% chance (0.05) that the means are actually the same, thereby rejecting our original hypothesis that they were.

## CHAPTER 6: CONCLUSION

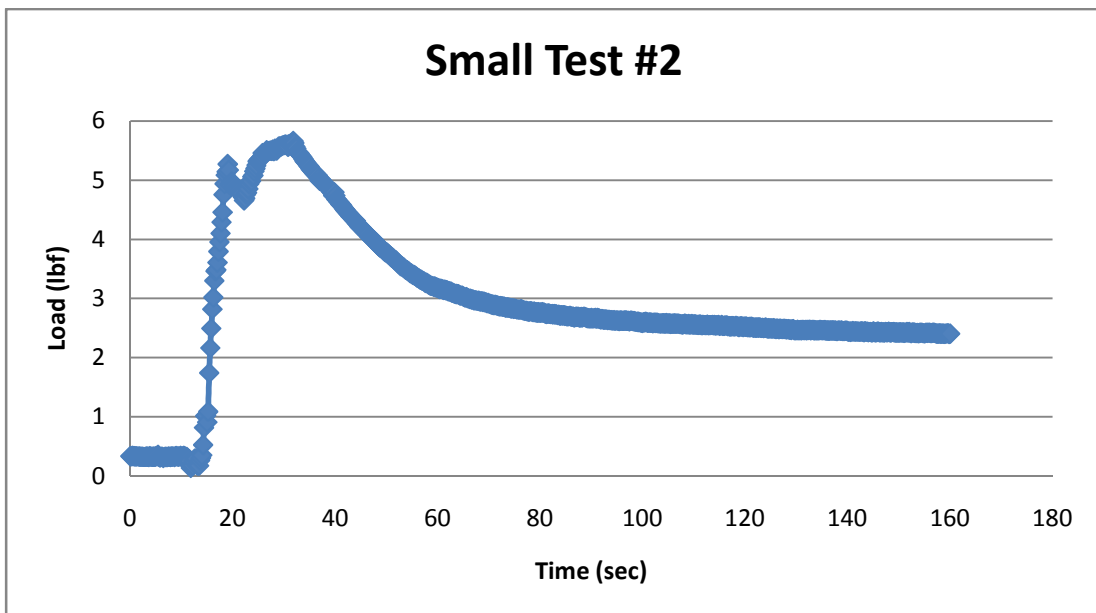
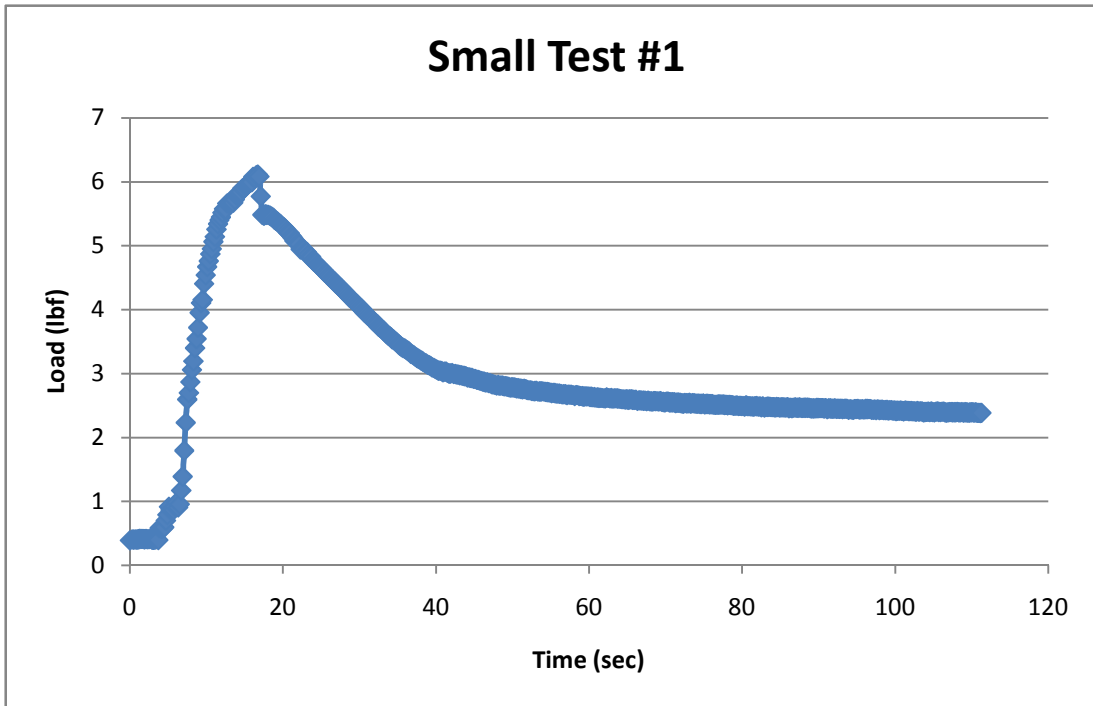
The purpose of this thesis was to measure the forces that were generated by various shape memory Nitinol implant staples in confined compression after the implant was transformed from martensite to austenite.

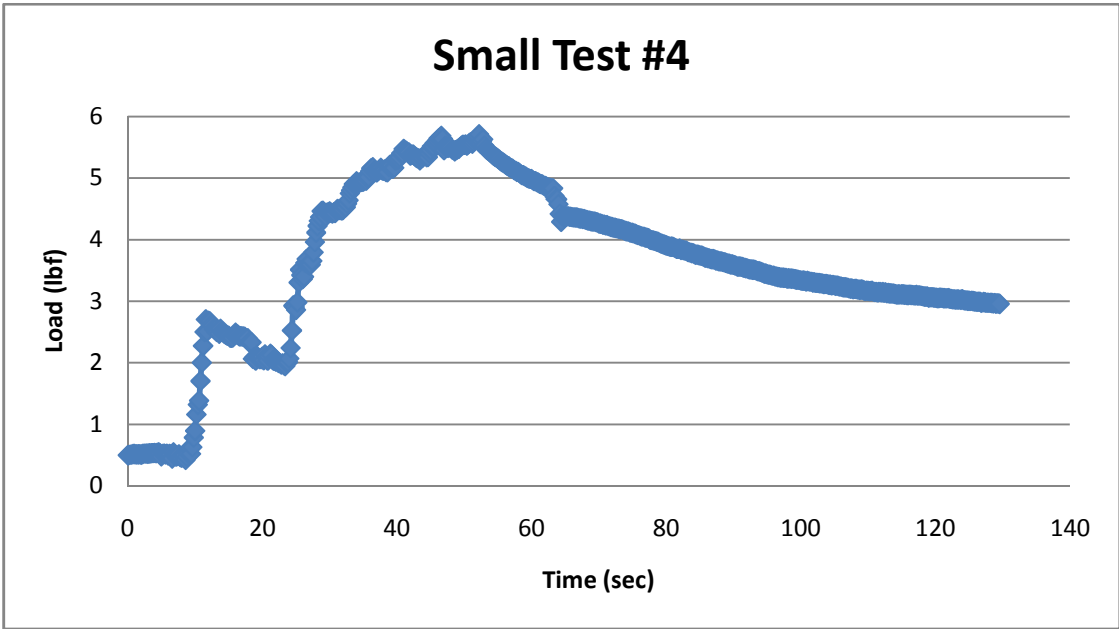
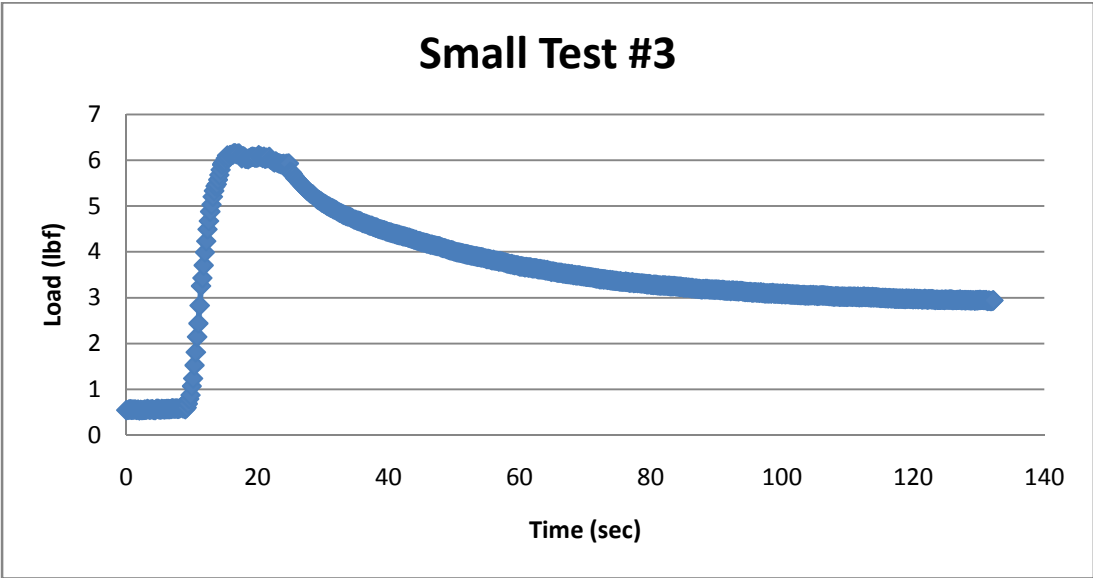
The small implants produced a mean force of  $2.8 \pm 0.28$  lbf, medium implants produced a mean force of  $3.6 \pm 0.17$  lbf, and large implants produced a mean force of  $7.3 \pm 0.40$  lbf. These dynamic forces are integral to bone healing. Relaying this information to orthopedic surgeons is important when determining the appropriate implant size selection. While the mean forces produced by these implants may seem too small to be applied for orthopedic surgery, these implants are mainly designed to be used only for small bones of the hand and feet, and as such do not require significantly large forces.

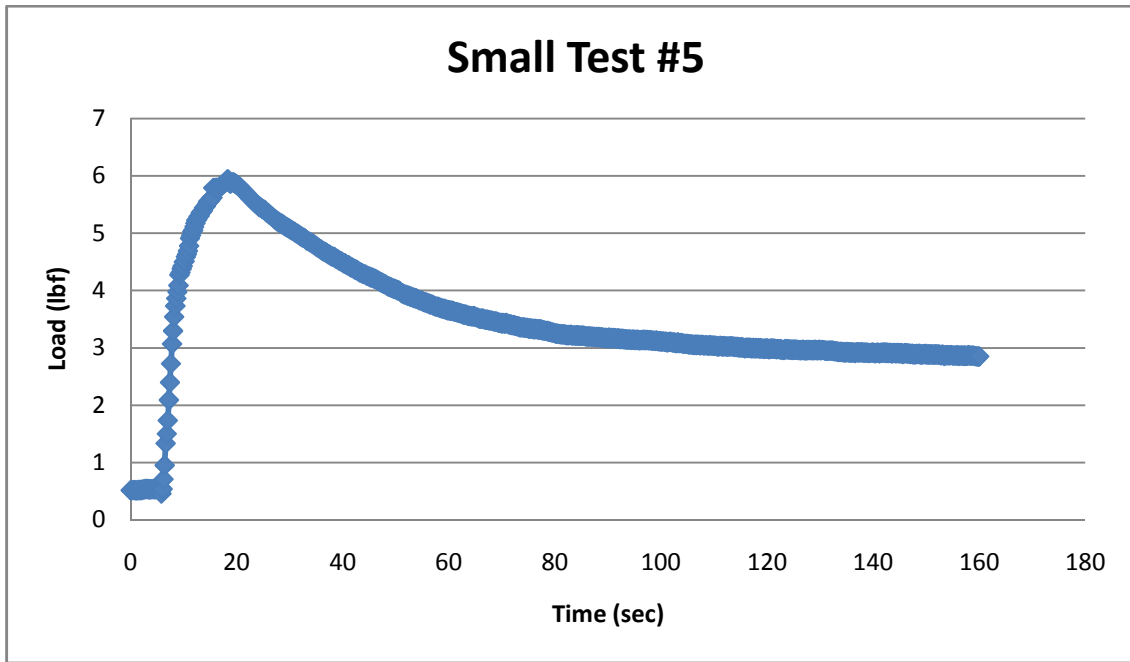
Implant manufacturers want to be able to accurately predict steady state loads by varying the gauge of the implant. While this experiment found these relationships to be non-linear, it is expected that testing done prior to the application of heat treatment may provide more linear results, and as such further testing in that area is required.

## APPENDIX I: LOAD VS TIME GRAPHS

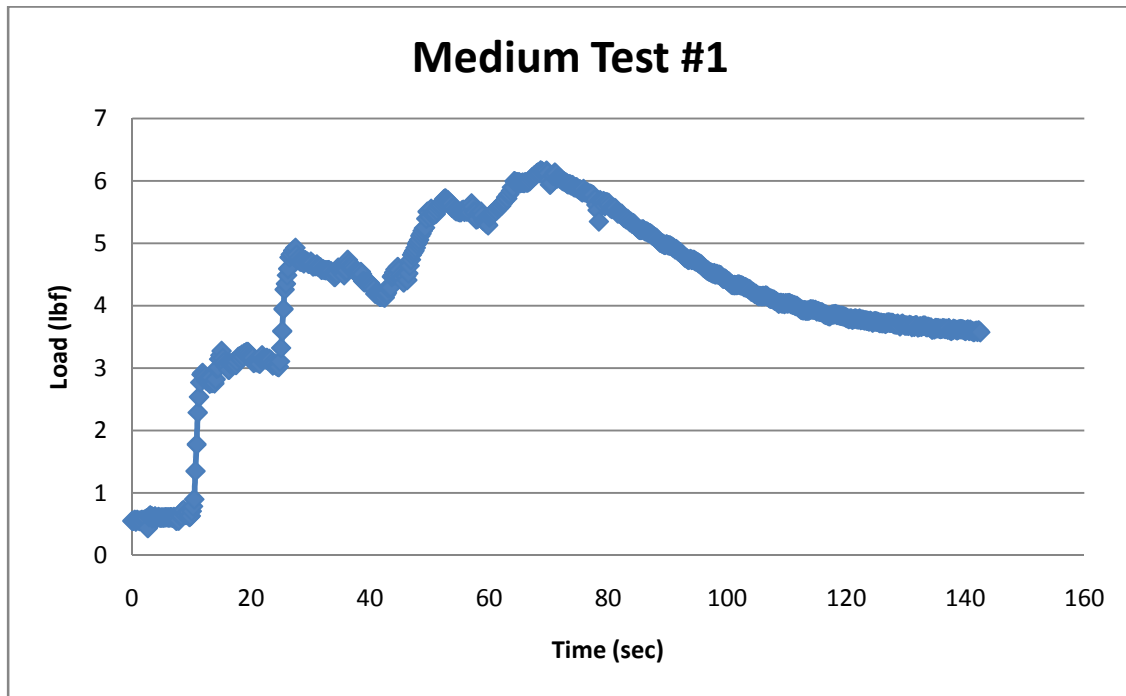
Figures A, B, and C contain the load vs. time graphs for Tests# 1 through 5 for the small, medium, and large staples, respectively.

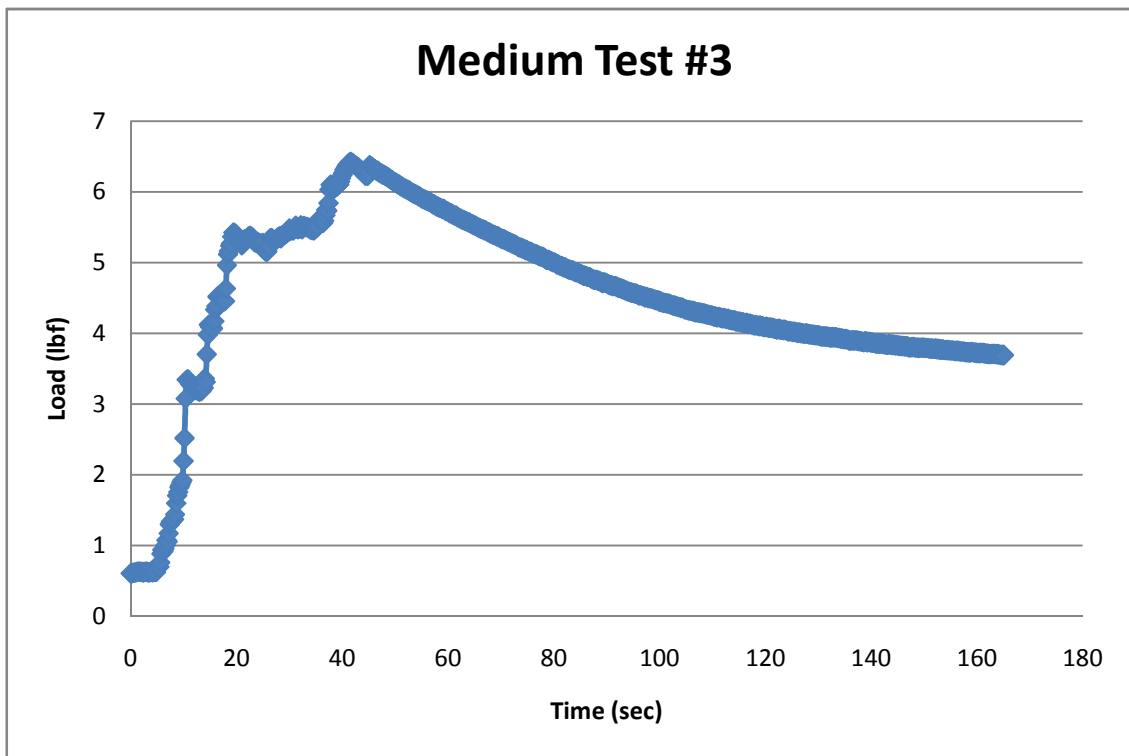
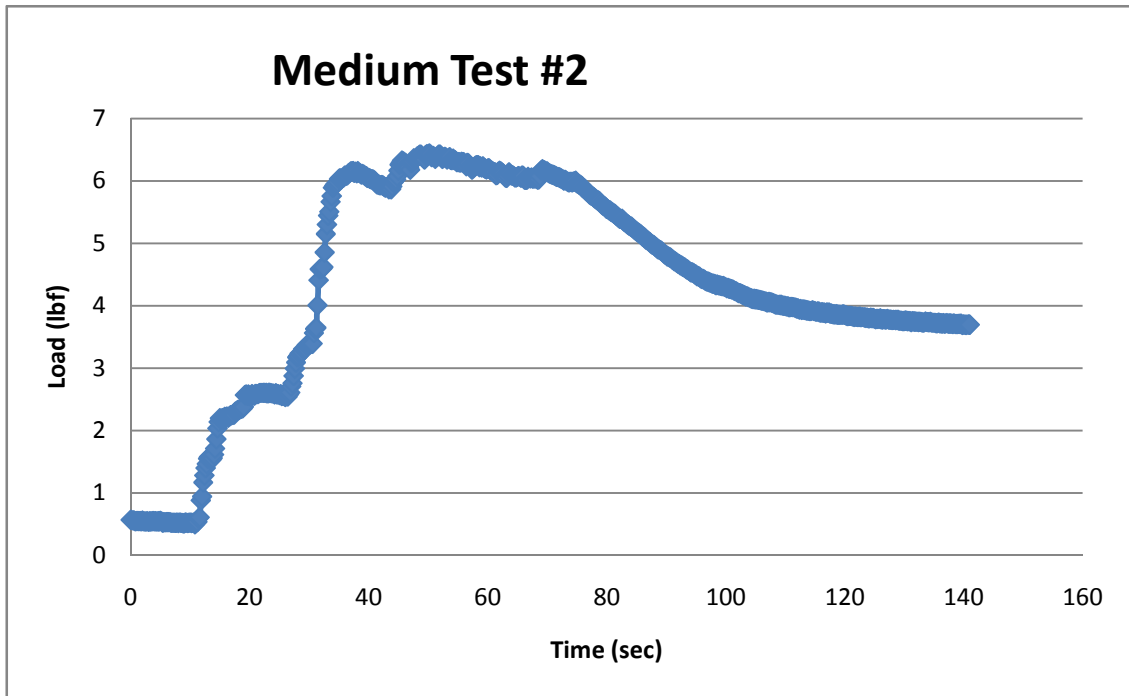


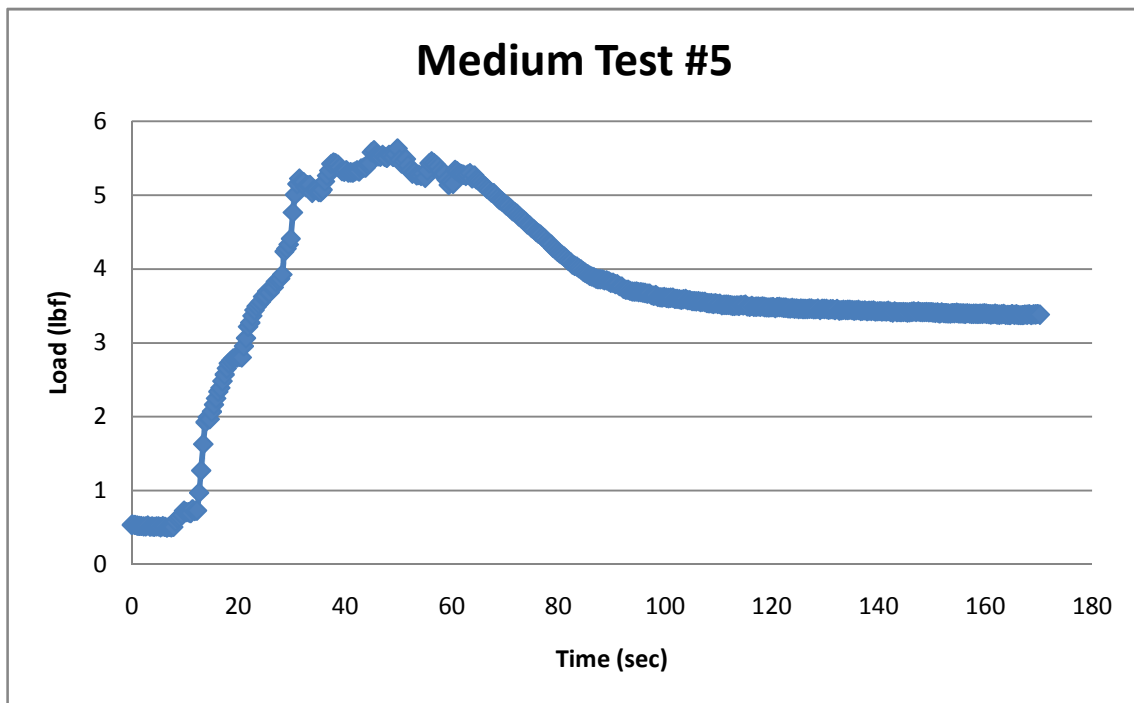
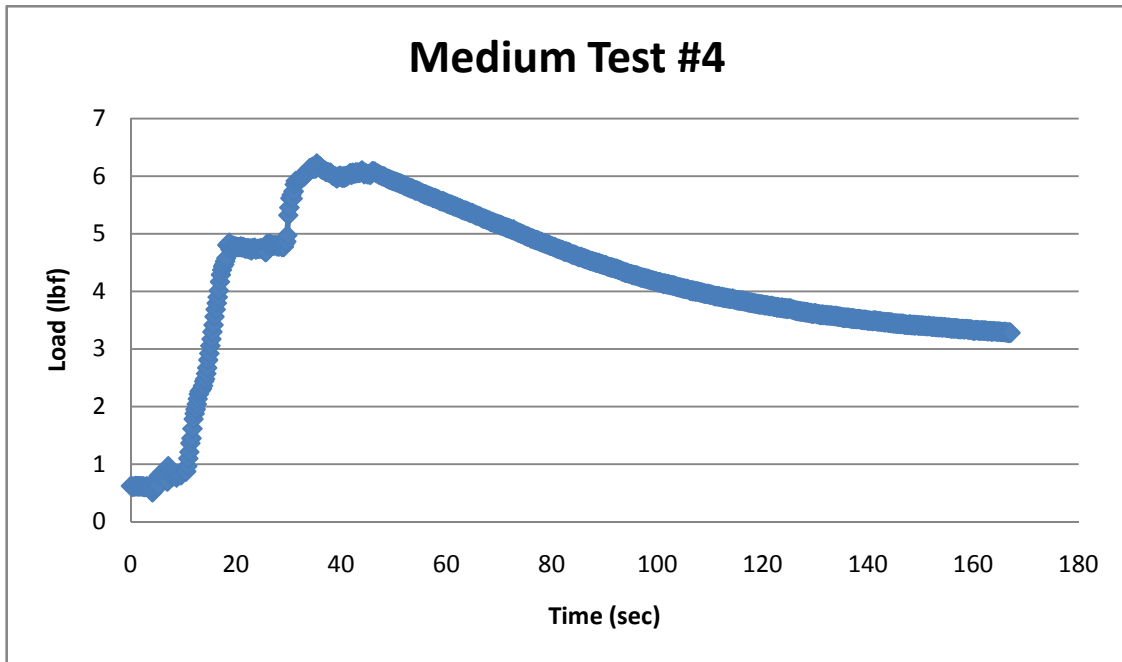




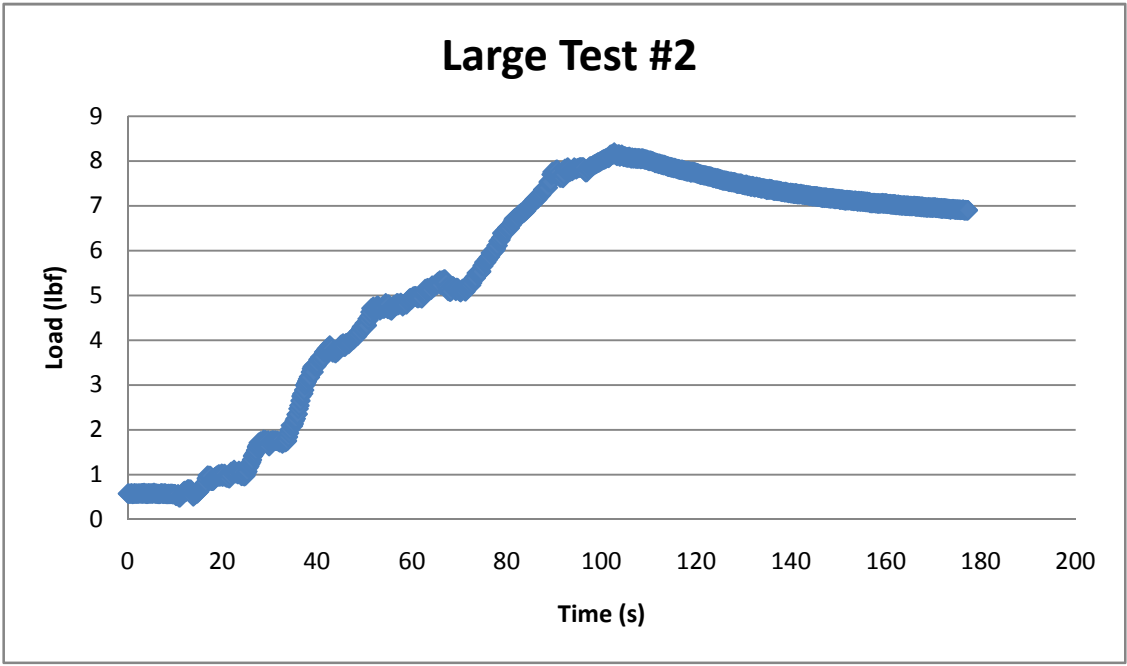
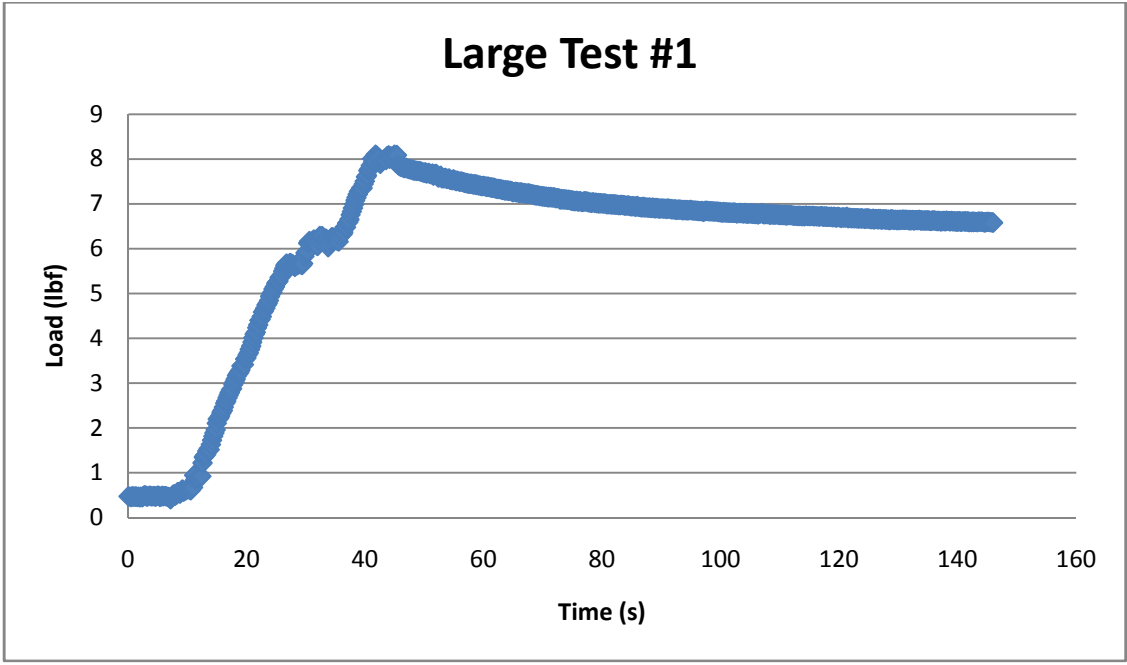
**Figure A:** Tests #1-5 for the small implants

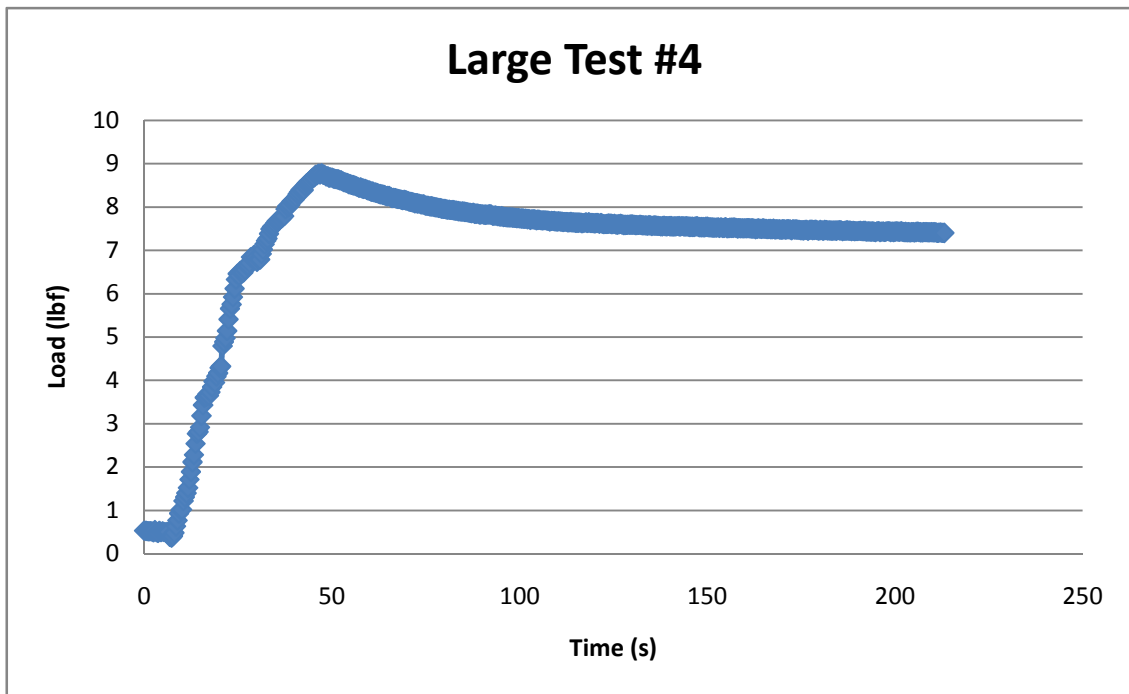
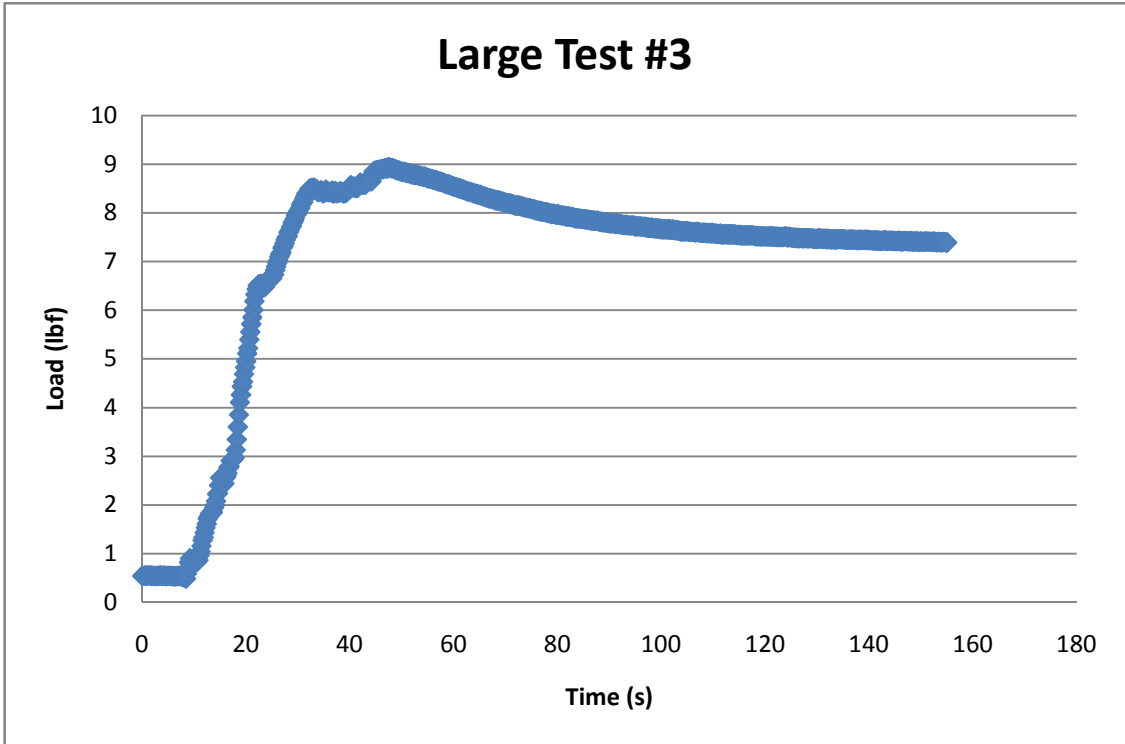






**Figure B:** Tests #1-5 for the medium implants





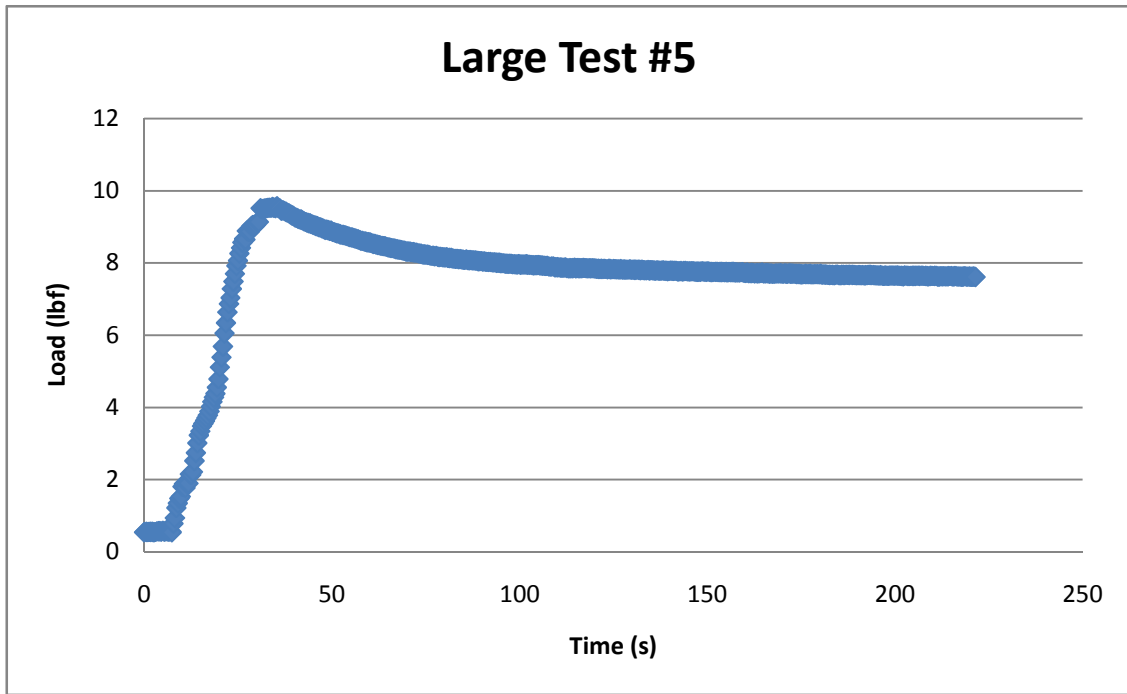


Figure C: Tests #1-5 for large implants

## APPENDIX II: MEASURED EXPERIMENTAL VALUES

Table A, B, and C is a list of the measured experimental values obtained from tests # 1-5 of the force generation of small, medium, and large staples.

<b>Table A: Measured Experimental Values of Small Implants (9x6x6 mm)</b>		
<b>Size / Test #</b>	<b>Peak Load (lbf)</b>	<b>Steady State (lbf)</b>
Small / 1	6.11	2.45
Small / 2	5.66	2.51
Small / 3	6.15	2.97
Small / 4	5.71	3.04
Small / 5	5.94	2.96

<b>Table B: Measured Experimental Values of Medium Implants (15x12x12 mm)</b>		
<b>Size / Test #</b>	<b>Peak Load (lbf)</b>	<b>Steady State (lbf)</b>
Medium / 1	6.17	3.62
Medium / 2	6.44	3.69
Medium / 3	6.43	3.87
Medium / 4	6.22	3.49
Medium / 5	5.63	3.43

<b>Table C: Measured Experimental Values of Large Implants (30x30x30 mm)</b>		
<b>Size / Test #</b>	<b>Peak Load (lbf)</b>	<b>Steady State (lbf)</b>
Large / 1	8.10	6.61
Large / 2	8.19	7.28
Large / 3	8.94	7.44
Large / 4	8.78	7.56
Large / 5	9.57	7.79

### APPENDIX III: PROOF OF NON-LINEAR RELATIONSHIP

The following is proof of the nonlinear relationship that exists when the steady state load is modeled as a simple beam in bending using  $\sigma = \frac{M*c}{I}$ :

$\sigma_{MAX}$  = constant max stress to bend staple at transformation temperature

$$\text{For } r=0.6 \text{ mm, } I = \frac{\pi*(r^4)}{4} = .102 \text{ mm}^4$$

$$\text{For } r=0.75 \text{ mm, } I = \frac{\pi*(r^4)}{4} = .249 \text{ mm}^4$$

$$\text{For } b=3 \text{ mm and } h=2 \text{ mm, } I = \frac{b*(h^3)}{12} = 2 \text{ mm}^4$$

Yield stress same for all implants since it's the same material, so take out  $\sigma$ .

$$M_{1.2} = \frac{11.2}{c} = \frac{.102}{.6} = .17 \text{ mm}^3$$

$$M_{1.5} = \frac{11.5}{c} = \frac{.249}{.75} = .332 \text{ mm}^3$$

$$M_{2X3} = \frac{12X3}{c} = \frac{2}{1} = 2 \text{ mm}^3$$

So, graphing moment for each implant in terms of mean steady state force:

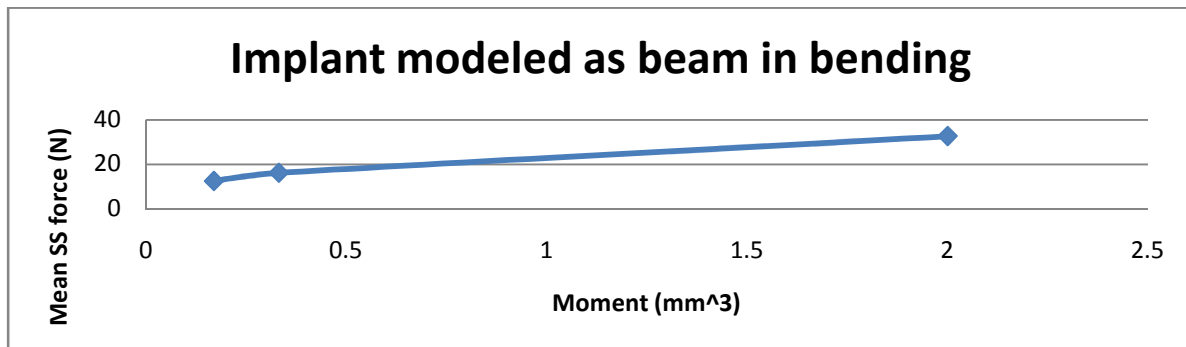


**Figure D:** Proof of non-linear relationship of sample when modeled as beam in bending

This clearly shows a non linear relationship for the sample when it is modeled as a beam in bending.

## REFERENCES

1. [Anonymous]. (2006). Retrieved on December 15, 2007, from <http://www.mts.com/en/Material/Dynamic/index.asp>
2. Cluett, J., M.D., Grossman, K., M.D. (2007). Retrieved on October 20, 2007, from <http://orthopedics.about.com/cs/otherfractures/a/fracture.htm>
3. Kapanen, A., Ryhanen, J., Danilov, A., Tuukkanen, J. (2001). Effect of nickel-titanium shape memory metal alloy on bone formation. *Biomaterials*, 22, 2475-2480.
4. Kauffman, G.B., Mayo, I. (1996). The story of nitinol: The serendipitous discovery of the memory metal and its applications. *The Chemical Educator*, 2(2), 1-21.
5. Kenneth J., Koval MD. (2002). Orthopaedic knowledge update 7: home study syllabus. *American Academy of Orthopedic Surgeons, New York, 1*.
6. Kujala, S. (2003). Biocompatibility and biomechanical aspects of nitinol shape memory metal implants. *Department of Surgery, University of Oulu*.
7. Kushner, A. (1940). Evaluation of wolff's law of bone formation. *The Journal of Bone & Joint Surgery*, 22, 589-596.
8. Machado, L.G., Savi, M.A. (2003). Medical applications of shape memory alloys. *Brazilian Journal of Medical and Biological Research*, 36(6), 683-691.
9. Moritz, A.R., Henriques, F.C. (1947). The relative importance of time and surface temperature in the causation of cutaneous burns. *Department of Legal Medicine*, 695-720.
10. Mureau, TM, DPM, Ford, TC, DPM. (2006). Nitinol compression staples for bone fixation in foot surgery. *Journal of the American Podiatric Medical Association*, 96(2), 102-6.
11. Musialek, J., Filip, P., Nieslanik, J. (1998). Titanium-nickel shape memory clamps in small bone surgery. *Arch Orthopedic Trauma Surgical*, 117, 341-344.
12. Praemer, A., Furner S., Rice DP. (1999). Musculoskeletal conditions in the united states. *American Academy of Orthopedic Surgeons, Rosemont, IL*.
13. Ryhänen, J., Kallioinen, M., Serlo, W., Perämäki, P., Junila, J., Sandvik, P., Niemelä, E., Tuukkanen, J. (1999). Bone healing and mineralization, implant corrosion, and and trace metals after nickel titanium shape memory metal intramedullary fixation. *J Biomed Mater*, 47, 472-480.

14. Shabalovskaya, S.A. (2001). Physicochemical and biological aspects of nitinol as a biomaterial. *International Materials Review*, 46(4), 1-18.
15. Shibuya, N., DPM, Manning, S.N., DPM, Meszaros, A., DPM, Budny, A.M., DPM, Malay, D. S., DPM, FACFAS, Yu, G. V., DPM, FACFAS. (2007). A compression force comparison study among three staple fixation systems. *The Journal of Foot & Ankle Surgery*, 46(1), 7-15.
16. Van Riet, R.P., MD, PhD, Bain, G. I., MBBS, FRACS. (2006). Three-corner wrist fusion using memory staples. *Techniques in Hand & Upper Extremity Surgery*, 10(4), 259-264.
17. Wayman, C.M., Duerig, T.W. (1990). An introduction to martensite and shape memory. *Engineering Aspects of Shape Memory Alloys*, 3-20.
18. Yetkin, H. MD, Kanatli, U., Senkoylu, A. MD, Cila, E. MD, Simsek, A. MD. (1999). Orthopedic applications of shape memory staples. *Gazi Medical Journal*, 10, 153-155.

## **BIOGRAPHY**

Jibin Mathew Mattappally (known as 'Jay Mattappally') was born in the city of Dubai, United Arab Emirates, on July 16, 1986, to Mathew and Mary Mattappally. Soon after his mother got a job at St. Vincent's Hospital in Jacksonville, Florida in 2000, he moved there with his family. He graduated from Robert E. Lee Senior High School in Jacksonville, Florida. He is currently a student of Tulane University in New Orleans, LA, majoring in Biomedical Engineering and minoring in Mathematics. He has been active in numerous clubs and organizations on campus such as the Tulane Biomedical Engineering Society (BMES), in which he has served a term as community service/social chair. He has been an ambassador to the Office of Multicultural Affairs (OMA) for the past two years and has actively participated in various community service events through his fraternity, Zeta Psi. During the summer of 2007, he had an internship with Intelifuse, Inc. in New Orleans, Louisiana, where he performed various operations duties like the inventory and inspection of various surgical implants, created an extensive database of literature articles suitable for future company research, and assisted in the shipping and packaging of implants. He plans on attending the Master of Engineering Management (MEM) program at Duke University in Durham, North Carolina, in the fall. After this program, he hopes to be involved in product design and management in a biomedical device company, culminating in executive management and other similar ventures in the future.